JACS
JOURNAL OF THE AMERICAN CHEMICAL SOCIETY

Communication

pubs.acs.org/JACS

Conductance Switching in the Photoswitchable Protein Dronpa

Katalin V. Korpany,[†] Pinky Langat,[†] Dong Myeong Kim,[†] Neil Edelman,[†] Daniel R. Cooper,[‡] Jay Nadeau,[‡] and Amy Szuchmacher Blum*,[†]

[†]Department of Chemistry, McGill University, 801 Sherbrooke Street West, Montreal, QC H3A 0B8, Canada

[‡]Department of Biomedical Engineering, McGill University, 3775 University Street, Montreal, QC H3A 2B4, Canada

Supporting Information

ABSTRACT: Dronpa, a photoswitchable GFP-like protein, was self-assembled onto gold substrates, and its conductance was measured using scanning tunneling microscopy (STM) and scanning tunneling spectroscopy (STS).

Fluorescent proteins have demonstrated tremendous utility in science as noninvasive imaging agents, especially in localizing proteins of interest within cells. Recently developed super-resolution imaging techniques such as PALM,[1] STORM,[2] and RESOLFT[3] rely on the ability to switch signals on and off, making switchable fluorescent proteins of great interest. In addition, reversibly switchable fluorescent proteins may further prove to be useful in novel applications in cell biology and opto-electronics. Such proteins can be repeatedly and reversibly switched between a fluorescent and a nonfluorescent state via irradiation at appropriate wavelengths, providing advantages in protein tracking and optical switching applications. Given that the chromophore in fluorescent proteins consists of aromatic moieties, it is possible that changes in fluorescence would be accompanied by changes in protein conductivity, leading to biologically based opto-electronic switches. Here, we measure the conductance of Dronpa, a reversibly photoswitchable green fluorescent protein (GFP) in the bright and dark states.

Dronpa is a monomeric engineered mutant of an oligomeric fluorescent protein found in *Pectiniidae* coral species.[4] Dronpa can be switched from a nonfluorescent "dark" state to an activated "bright" state when illuminated with 405 nm light; exposure to 488 nm light returns it to the dark state. The process may be repeated dozens of times without photobleaching of the protein.[5] The tertiary structure of Dronpa (Figure 1A) closely resembles that of typical GFPs and related proteins. The chromophore forms spontaneously from the Cys 62-Tyr 63-Gly 64 tripeptide residues in an α-helical segment that is coaxially threaded through the β-barrel.[6] The precise molecular mechanism of Dronpa photoswitching is not completely understood. Photoswitching is thought to be a result of both the photoinduced protonation/deprotonation[5,7] and the cis−trans isomerization of the chromophore.[6,8] The fluorescent on-state of Dronpa (bright state) has the chromophore in cis-conformation within the β-barrel, and the nonfluorescent off-state (dark state) chromophore possesses a trans-conformation (Figure 1B, C).

The $I-V$ characteristics of conductive proteins have been examined in several studies, but rarely at the single-molecule level. STM and STM-based techniques allow for single-molecule resolution of molecular charge transport, in contrast to other methods such as cyclic voltammetry that only provide information on the average behavior of an ensemble of molecules. STM has been successfully used to study the electronic properties of conductive proteins such as cytochrome,[9−12] cytochrome GFP fusion proteins,[13] GFP−cytochrome *c* heteroprotein layers,[14−17] ferritin,[18] photoactive yellow protein (PYP),[19] and azurin.[20] To our knowledge, there have been no STM or STS studies regarding the fluorescent protein Dronpa.

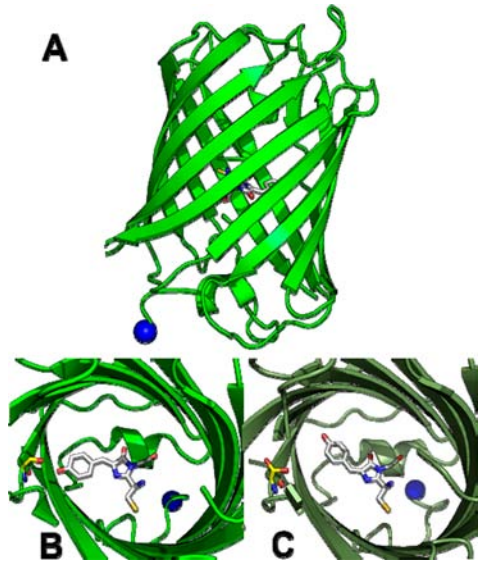

Figure 1. (A) Structure of bright state Dronpa (PDB ID: 2Z1O) with N-terminus highlighted in blue. The chromophore, in white, resides in the center of the β-barrel. Upon photoswitching from the (B) bright state to the (C) dark state (PDB ID: 2POX), the chromophore adopts a trans conformation and loses some stabilizing hydrogen-bonding contacts (e.g., Ser142, in yellow) following a cascade of residue rearrangements within the barrel.[6] Structural models were generated using PyMOL (v. 1.4.1) with structural data provided by RCSB Protein Data Bank (www.rcsb.org).

In order to better understand the optoelectronic properties of this reversibly photochromic protein, we measured the conductance of Dronpa protein self-assembled onto gold substrates using STM and STS. The effect of molecular

Received: June 20, 2012
Published: September 11, 2012

   dx.doi.org/10.1021/ja306031n | *J. Am. Chem. Soc.* 2012, 134, 16119−16122

orientation on conductance was investigated by comparing measurements from an N-terminal 6xHN-tagged Dronpa (HT-Dronpa) and a variant in which the tag had been removed by enzymatic cleavage (HC-Dronpa) (Supporting Information, Figure S1). Histidine tags are routinely used in the purification of proteins by affinity chromatography but may also be used as chemical handles to attach peptides and proteins to various surfaces via chelator groups,[21] thereby controlling their orientation. Assembly of histidine-tagged molecules on bare gold,[22] without the presence of chelator groups, is possible and appears to be mediated by the imidazole of the His residues. Molecular dynamics (MD) simulations and DFT calculations also predict high binding affinity of histidine for Au(111) surfaces.[23,24]

Briefly, protein monolayers were formed on Au(111) substrates (Supporting Information, [SI]) and characterized by STM. It is clear from the STM imaging (Figure 2) that HT-Dronpa forms more uniform monolayers on gold than HC-Dronpa, likely due to the presence of the 6xHN tag influencing deposition. Higher-resolution images of the HT-Dronpa monolayer (Figure 2, Inset A; SI, Figure S2) reveal the measured diameter of HT-Dronpa on gold is ~3 nm. This value corresponds well to the dimensions of Dronpa, which measures 3.8 nm × 3.2 nm × 5.4 nm, based on X-ray crystallographic data (PDB ID: 2POX) (SI, Figure S2). Isolated monomers of HC-Dronpa are shown in SI, Figure S3, showing measured diameters of ~5 nm. Fluorescence measurements performed on HT-Dronpa monolayers show emission at 522 nm (SI, Figure S4), confirming that the protein is still fluorescent and thus likely remains intact.[25]

To investigate the effect of photoswitched state on conductance, Dronpa monolayers on Au(111) were measured by STM and STS after the protein was reversibly switched to a nonfluorescent dark state and to the fluorescent bright state in a cyclic fashion using 488 and 405 nm light, respectively (SI). To ensure that Dronpa was photoswitched under these conditions, UV−vis spectroscopy was used to confirm the state of the protein in solution after illumination (SI, Figure S5). *I*−*V* measurements obtained by STS were averaged for each photostate and plotted for comparison (Figure 3). For each photostate, resistance was calculated as the inverse slope of the linear fit of the Ohmic region (−0.1 V to +0.1 V) of the averaged *I*−*V* measurements for that state (Table 1). Dronpa spectra were consistent with a resistive tunneling junction and were generally symmetric (Figure 3). Tunneling spectra for both HT and HC-Dronpa appear to be exponential in form, as expected for direct tunneling between tip and sample with the protein acting as a barrier in between. The absence of distinct features at particular applied bias voltages suggests that tunneling is elastic and does not involve specific orbitals on the protein. Ambient-state resistance was very similar to the observed bright-state resistance values for both HT and HC-Dronpa. This was consistent with the observation that Dronpa at equilibrium is typically in the bright state.[8] Conductance did vary with the photoswitched state for HT-Dronpa. The dark-state Dronpa was more conductive than that of the bright or ambient state for HT-Dronpa. Although the specific mechanism of conductance in proteins is still unclear,[19] changes in

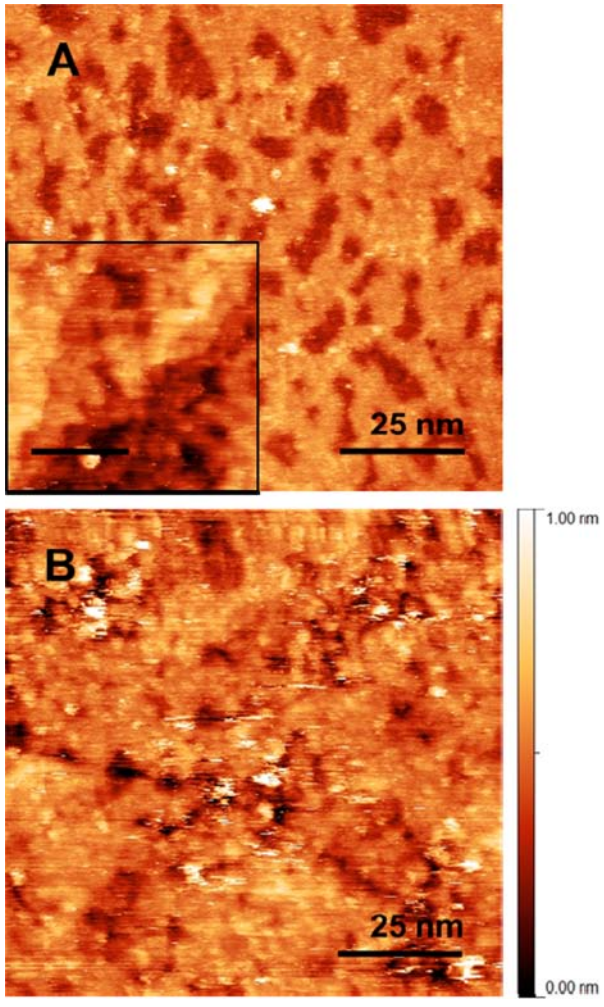

Figure 2. STM imaging of (A) HT-Dronpa (set point: 160 pA) and (B) HC-Dronpa (set point: 160 pA) on Au(111). (Inset A) Higher-resolution image of HT-Dronpa (set point: 250 pA, scale bar: 20 nm). Bias voltage was 1 V for all images. The 6xHN tag of HT-Dronpa facilitates the formation of more ordered self-assembled monolayers of protein, in comparison to HC-Dronpa.

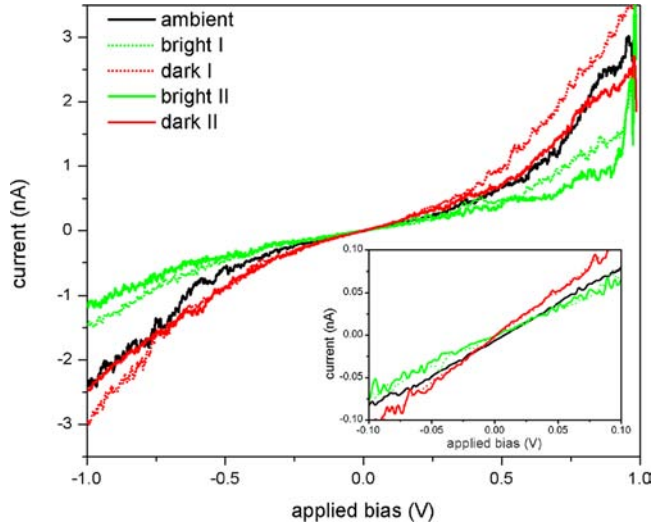

Figure 3. Averaged STS *I*−*V* spectra of HT-Dronpa as the protein is cycled through dark and bright states. Spectra were obtained by measuring current while the bias voltage is swept from −1 V to +1 V, using a trigger point of 15 pA. (Inset) Ohmic region (−0.1 V to +0.1 V) of *I*−*V* spectra of HT-Dronpa. An increase in conductance is visible upon switching from the bright state to the dark state.

dx.doi.org/10.1021/ja306031n | J. Am. Chem. Soc. 2012, 134, 16119−16122

Table 1. Summary of STM Resistances[a] for HT-Dronpa and HC-Dronpa

sample	ambient (GΩ)	N[c]	dark I (GΩ)	N	bright I (GΩ)	N	dark II (GΩ)	N	bright II (GΩ)	N
HT-Dronpa[b]	1.80 ± 0.01	68	0.487 ± 0.003	84	1.99 ± 0.04	128	–		–	
	1.139 ± 0.009	136	0.506 ± 0.002	160	1.461 ± 0.006	140	0.561 ± 0.004	72	–	
	1.194 ± 0.007	72	0.915 ± 0.003	112	1.42 ± 0.01	120	0.910 ± 0.007	100	1.52 ± 0.02	100
	1.72 ± 0.01	132	0.56 ± 0.02	68	1.94 ± 0.02	88	0.575 ± 0.003	116	2.14 ± 0.01	72
HC-Dronpa	0.404 ± 0.006	115	0.399 ± 0.003	112	0.356 ± 0.004	88	–		–	
	0.439 ± 0.003	120	0.517 ± 0.004	116	0.3131 ± 0.009	104	–		–	

[a]Resistance is calculated from the slope of the linear fit of the Ohmic region (−0.1 to +0.1 V). [b]Each row of the table corresponds to a separate sample. [c]*N* denotes the number of *I*−*V* spectra used for the calculation of STM resistances for each sample and photostate.

conduction between the bright and dark states indicated that the structural conformation of the protein was of critical importance in transport through proteins. In the dark state, the chromophore switches to a trans conformation, causing changes in the type and number of amino acid close contacts, which could explain our findings. This difference in resistance was not seen in the HC-Dronpa samples. This suggests that the chromophore was involved in the tunneling path for the HT-Dronpa, but not in the HC-Dronpa, probably due to orientation effects. For samples in which the photoswitching cycle is repeated, the bright and dark state resistances are reproducible.

Dependence of molecular orientation on conductance was investigated by comparing resistance values between HT and HC-Dronpa for protein in the same photoswitched state. On the basis of STM imaging, the 6xHN tag in HT-Dronpa conferred directionality to the protein monolayer, as HC-Dronpa films appeared less regular and more disorganized. Certain residues in HC-Dronpa may have influenced deposition. The strongest binding to Au would be expected from Cys residues, of which wild-type Dronpa possesses three, but only CYS113 is solvent-exposed and able to participate in binding to Au(111). It is thus more likely that other residues were responsible for the orientation; the high concentration of aromatic His and Phe residues on one face of the β-barrel are expected to have strong affinity for the gold substrate (SI, Figure S6). Previous computational studies have calculated the interaction free energy of the noncovalent association of amino acids with Au(111).[23] The relative binding affinity of His (34.0 kJ/mol) was found to be slightly lower than that of Cys (37.7 kJ/mol). Of all amino acids under study, Phe possessed the second most favorable interaction with gold at 43.6 kJ/mol.

The strong affinity of His and Phe for Au(111) would encourage the protein to lie down, in contrast to the vertical alignment expected in the HT-Dronpa case. Thus, the difference in the resistance values between the two proteins could be attributed to a different alignment of the chromophore, as the protein is being interrogated from different angles. Differences in conductance with protein orientation relative to the substrate have also been observed for cytochrome b_{562}.[26] These differences were shown to depend on whether the protein was immobilized vertically on Au(111) or assembled with its long axis parallel to the substrate. We observe a difference in measured diameter for the two samples (3 nm for HT-Dronpa vs 5 nm for HC-Dronpa) that is consistent with differences in the alignment of the protein barrel. However, although the data shows that the presence of the 6xHN tag has a strong effect on the contact point between the protein and the substrate, the relatively broad spread in the measured resistance shown in histograms of the STS data (SI, Figure S7) indicates that the high degree of flexibility at the protein terminus means that the 6xHN tag does not fully control protein orientation with respect to the substrate.

In summary, we have studied the conductance of HT and HC-Dronpa monolayers on Au(111) using STM and STS. The addition of a 6xHN tag, initially introduced to aid in purification, resulted in better self-assembled monolayers of protein on gold. This observation may be useful for those hoping to increase the quality of monolayer deposition of proteins on gold substrates. Differences in conductance between HT and HC-Dronpa revealed the importance of protein structural conformation, and the effect of molecular orientation, on electron transport through proteins. Conductance was found to significantly increase upon photoswitching HT-Dronpa from dark to bright state. This demonstration of reversibly photoswitching conductance in HT-Dronpa represents an important step in achieving biologically based opto-electronic molecular switches.

■ ASSOCIATED CONTENT

Supporting Information

Details of experimental procedures; protein sequence of HT-Dronpa construct (Figure S1); STM higher resolution of HT-Dronpa (Figure S2); STM higher resolution of HC-Dronpa (Figure S3); fluorescence emission spectrum of HT-Dronpa (Figure S4); UV−visible spectroscopy of Dronpa photoswitching (Figure S5); proposed orientation of HT and HC-Dronpa on Au(111) (Figure S6); histograms of resistances of individual *I*−*V* spectra (Figure S7). This material is available free of charge via the Internet at http://pubs.acs.org.

■ AUTHOR INFORMATION

Corresponding Author

amy.blum@mcgill.ca

Funding

This work was supported by the Natural Sciences and Engineering Research Council of Canada (NSERC) and the Canada Foundation for Innovation (CFI). D.R.C. was supported by the Systems Biology Training Program.

Notes

The authors declare no competing financial interest.

■ ACKNOWLEDGMENTS

Assistance from Tim Gonzalez of the Department of Chemistry for the protein irradiation is gratefully acknowledged.

■ REFERENCES

(1) Betzig, E.; Patterson, G. H.; Sougrat, R.; Lindwasser, O. W.; Olenych, S.; Bonifacino, J. S.; Davidson, M. W.; Lippincott-Schwartz, J.; Hess, H. F. *Science* **2006**, *313*, 1642.

(2) Rust, M. J.; Bates, M.; Zhuang, X. W. *Nat. Methods* **2006**, *3*, 793.

(3) Hofmann, M.; Eggeling, C.; Jakobs, S.; Hell, S. W. *Proc. Natl. Acad. Sci. U.S.A.* **2005**, *102*, 17565.
(4) Ando, R.; Mizuno, H.; Miyawaki, A. *Science* **2004**, *306*, 1370.
(5) Habuchi, S.; Dedecker, P.; Hotta, J. I.; Flors, C.; Ando, R.; Mizuno, H.; Miyawaki, A.; Hofkens, J. *Photochem. Photobiol. Sci.* **2006**, *5*, 567.
(6) Andresen, M.; Stiel, A. C.; Trowitzsch, S.; Weber, G.; Eggeling, C.; Wahl, M. C.; Hell, S. W.; Jakobs, S. *Proc. Natl. Acad. Sci. U.S.A.* **2007**, *104*, 13005.
(7) Wilmann, P. G.; Turcic, K.; Battad, J. M.; Wilce, M. C. J.; Devenish, R. J.; Prescott, M.; Rossjohn, J. *J. Mol. Biol.* **2006**, *364*, 213.
(8) Stiel, A. C.; Trowitzsch, S.; Weber, G.; Andresen, M.; Eggeling, C.; Hell, S. W.; Jakobs, S.; Wahl, M. C. *Biochem. J.* **2007**, *402*, 35.
(9) Della Pia, E. A.; Chi, Q. J.; Jones, D. D.; Macdonald, J. E.; Ulstrup, J.; Elliott, M. *Nano Lett.* **2011**, *11*, 176.
(10) Wigginton, N. S.; Rosso, K. M.; Lower, B. H.; Shi, L.; Hochella, M. F. *Geochim. Cosmochim. Acta* **2007**, *71*, 543.
(11) Wigginton, N. S.; Rosso, K. M.; Hochella, M. F. *J. Phys. Chem. B* **2007**, *111*, 12857.
(12) Morimoto, J.; Tanaka, H.; Kawai, T. *Surf. Sci.* **2005**, *580*, L103.
(13) Lee, B.; Takeda, S.; Nakajima, K.; Noh, J.; Choi, J.; Hara, M.; Nagamune, T. *Biosens. Bioelectron.* **2004**, *19*, 1169.
(14) Choi, J. W.; Nam, Y. S.; Jeong, S. C.; Lee, W. H.; Petty, M. C. *Curr. Appl. Phys.* **2006**, *6*, 839.
(15) Choi, J. W.; Park, S. J.; Nam, Y. S.; Lee, W. H.; Fujihira, M. *Colloid Surf., B* **2002**, *23*, 295.
(16) Oh, S. Y.; Park, J. K.; Ko, C. B.; Choi, J. W. *Biosens. Bioelectron.* **2003**, *19*, 103.
(17) Choi, J. W.; Fujihira, M. *Appl. Phys. Lett.* **2004**, *84*, 2187.
(18) Rakshit, T.; Mukhopadhyay, R. *Langmuir* **2011**, *27*, 9681.
(19) Rzeznicka, I. I.; Wurpel, G. W. H.; Bonn, M.; van der Horst, M. A.; Hellingwerf, K. J.; Matsunaga, S.; Yamada, T.; Kawai, M. *Chem. Phys. Lett.* **2009**, *472*, 113.
(20) Davis, J. J.; Wrathmell, C. L.; Zhao, J.; Fletcher, J. *J. Mol. Recognit.* **2004**, *17*, 167.
(21) Kroger, D.; Liley, M.; Schiweck, W.; Skerra, A.; Vogel, H. *Biosens. Bioelectron.* **1999**, *14*, 155.
(22) Kogot, J. M.; England, H. J.; Strouse, G. F.; Logan, T. M. *J. Am. Chem. Soc.* **2008**, *130*, 16156.
(23) Hoefling, M.; Iori, F.; Corni, S.; Gottschalk, K. E. *Langmuir* **2010**, *26*, 8347.
(24) Iori, F.; Corni, S.; Di Felice, R. *J. Phys. Chem. C* **2008**, *112*, 13540.
(25) Schmid, E. L.; Keller, T. A.; Dienes, Z.; Vogel, H. *Anal. Chem.* **1997**, *69*, 1979.
(26) Della Pia, E. A.; Elliott, M.; Jones, D. D.; Macdonald, J. E. *ACS Nano* **2012**, *6*, 355.